

Mechanical damping and dynamic modulus measurements in alumina and tungsten fibre-reinforced aluminium composites

ALAN WOLFENDEN

Mechanical Engineering Department and Amorphous Materials Research Group, Texas A&M University, College Station, TX 77843, USA

JEFFREY M. WOLLA

Composites and Ceramics Branch (Code 6372), Materials Science and Technology Division, Naval Research Laboratory, Washington, DC 20375, USA

Simultaneous measurements of mechanical damping, or internal friction (Q^{-1}), and dynamic Young's modulus (E) were made near 80 kHz and at strain amplitudes (ε) in the range 10^{-8} to 10^{-4} on small specimens of continuous or chopped fibre-reinforced metal matrix composites (MMCs): 6061 aluminium reinforced with alumina (Al/Al₂O₃) and 6061 aluminium reinforced with tungsten (Al/W). Baseline experiments were also done on 99.999% aluminium (pure Al). The strain amplitude dependence of damping and the temperature dependence of dynamic modulus were of particular interest in this study. The temperature (T) dependence of the modulus from room temperature up to 475°C was determined for the Al/Al₂O₃ and pure Al specimens and a highly linear decrease in modulus with increasing temperature was observed. The rate of modulus loss ($dE/dT \approx -80 \text{ MPa}^\circ\text{C}^{-1}$) was the same for both materials and the reduction in modulus of the Al/Al₂O₃ was attributed to the reduction in modulus of the aluminium matrix, not the alumina fibres. The size, type, and amount of fibre reinforcement were found to have a significant effect on the strain amplitude dependence of the damping in both MMCs. Unreinforced aluminium exhibited classical dislocation damping trends with a region of strain amplitude independent damping at low strains (less than 10^{-5}) followed by a non-linear, strain amplitude dependent region at higher strains. The addition of alumina fibres (chopped or continuous), while increasing stiffness, resulted in a significant reduction in damping capacity for the MMC relative to that for aluminium and near complete suppression of the amplitude dependent response. The damping levels increased as the volume fraction of fibre, and therefore, the amount of fibre/matrix (FM) interface decreased, indicating that the matrix, not factors such as increased dislocation densities at the FM interface, was the dominant influence on the damping. Analysis of the Al/Al₂O₃ results by Granato-Lücke (GL) theory indicated that dislocation densities were increased relative to those in aluminium, but the dislocations were well pinned and unable to increase damping levels effectively. Analysis of the Al/W results by GL theory also revealed high dislocation densities, but, unlike the Al/Al₂O₃ specimens, the Al/W specimens (continuous fibres) exhibited strong amplitude dependent damping (starting near strain levels of 2×10^{-6}) with damping levels approximately twice those of pure aluminium. Trends showed increased damping with increased fibre diameter, not with increased FM interface area. There was some evidence that it was the tungsten fibre itself that dominated the damping behaviour in Al/W composites, not the aluminium matrix or the FM interface.

1. Introduction

In recent years, the materials requirements for advanced structural systems have driven research towards developing new lightweight, high-performance materials. Metal matrix composites (MMCs) have proved to be one class of materials capable of satisfying both the need for structural efficiency (high stiffness/weight and strength/weight ratios) and extreme environment survivability. More recently, the need for materials

with improved damping capacity, while maintaining the high-modulus and high-strength characteristics of the material, has become an increasingly more important design goal. An efficient means of meeting this goal would be to improve the intrinsic damping of MMCs. With these concerns in mind, a detailed study of the damping capacity and modulus of these materials was undertaken.

There are numerous factors to be considered in a

TABLE I Inventory of Al/W specimens

Fibre volume fraction (%)	Fibre diameter (mm)	Quantity	Label
36	0.305	1	Al/36W (0.305)
37	0.305	1	Al/37W (0.305)
44	0.127	1*	Al/44W (0.127)
46	0.305	2	Al/46W (0.305)
49	0.127	1	Al/49W (0.127)
50	0.127	1	Al/50W (0.127)
50	0.762	2	Al/50W (0.762)
55	0.305	2	Al/55W (0.305)

*Manufactured by DWA Composite Specialities. All others manufactured by TRW.

complete study of damping and modulus in MMCs and this study concentrated on two major areas. First, the dependence of the damping, or internal friction (Q^{-1}), on the strain amplitude (ϵ) of vibration was examined. Through this it was hoped that some insight could be gained as to which damping mechanisms are active in MMCs and how the structure and composition of MMCs affected these intrinsic damping mechanisms. Particular attention was paid to a dislocation damping theory proposed by Granato and Lücke [1, 2]. The second major area of study was the dependence of the dynamic modulus (E) of MMCs on temperature (T). This was of importance as many advanced materials will be required to withstand high-temperature operating conditions.

To accomplish the above objectives an apparatus known as the Piezoelectric Ultrasonic Composite Oscillator Technique (PUCOT), equipment that allows simultaneous measurements of the mechanical damping and dynamic modulus of relatively small specimens as a function of temperature, was used. The MMCs studied were 6061 aluminium (Al) reinforced with alumina (Al_2O_3) fibres, or Al/ Al_2O_3 , and 6061 aluminium reinforced with tungsten (W) fibres, or Al/W. In addition to studying the strain amplitude and temperature dependencies of the properties, the effects of fibre volume fraction, fibre diameter, and fibre form (continuous or chopped) were examined.

2. Experimental procedure

2.1. Materials

The specimens of Al/ Al_2O_3 were manufactured by DuPont and had either continuous or chopped 20 μ m diameter fibres in volume percentages of 30 (chopped), or 30, 45, and 55 (continuous). The Al/W specimens were manufactured either by TRW or by DWA Composite Specialities with fibre diameters of 0.127, 0.305, or 0.762 mm and fibre volume percentages between 36% and 55%. Table I shows an inventory of the Al/W specimens. A specimen of 99.999% aluminium (pure Al) was also tested to serve as a baseline for comparisons with the results from the MMCs.

All the specimens used, except the chopped fibre Al/ Al_2O_3 specimen, were cylindrical in shape and unidirectionally reinforced (fibres aligned parallel to cylinder axis). The chopped fibre sample was also cylindrical, but had a random fibre orientation. All of the specimens were typically 5 mm diameter and approximately 30 mm long (length varied according to

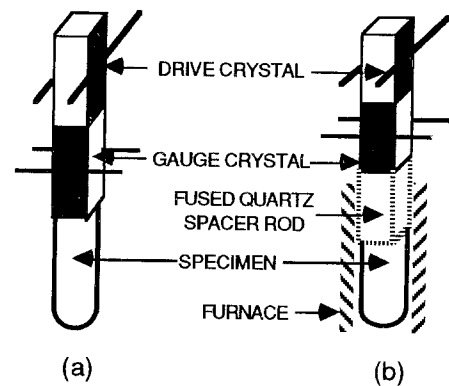


Figure 1 Schematic diagram of the piezoelectric ultrasonic composite oscillator technique (PUCOT) for measurements of damping and dynamic Young's modulus at (a) room temperature, and (b) elevated temperature.

resonant wavelength for the material as will be discussed in the next section).

2.2. PUCOT

The PUCOT has been described in detail previously [3, 4], but a brief description will be given here, because the technique is not well known. The basic features of the apparatus are shown in Fig. 1. The setup consisted of two piezoelectric quartz crystals, known as the drive (D) and the gauge (G) crystals, and the specimen (S), all joined by Loctite glue. When the drive crystal was excited with suitable alternating voltages, and the specimen was of appropriate resonant length, longitudinal, resonant, ultrasonic stress waves were produced in the specimen. The gauge crystal acted as a strain gauge in the system. It is emphasized that the stress waves were standing waves and the technique is not to be confused with the better known pulse-echo technique.

For measurements at room temperature, the three-component system (DGS) was used. For measurements at elevated temperatures, the four component system (DGQS) was needed, where Q denotes a fused quartz spacer rod tuned for resonance at particular temperatures. The system was driven at resonance by a closed loop oscillator which maintained a constant (user selectable) gauge crystal voltage, and hence, a known constant maximum strain (or stress) amplitude in the specimen. During typical tests, the values of the crystal voltages, and the resonant period of the DGS or DGQS system were measured. These measured values, along with other system constants, permitted the calculation of mechanical damping, maximum strain amplitude, and dynamic Young's modulus from standard PUCOT equations [3, 4]. For elevated temperature testing, the changes in density and length of the specimen due to heating were taken into account in the equations by incorporating the coefficient of thermal expansion of the specimen.

The procedure for determining the strain amplitude dependence of damping involved selecting numerous values of the gauge crystal voltage in the range from 1 mV to 10 V, corresponding to strains from 2×10^{-8} to 3×10^{-4} for these materials. At each setting the drive crystal voltage and the resonant period were recorded to enable a separate determination of

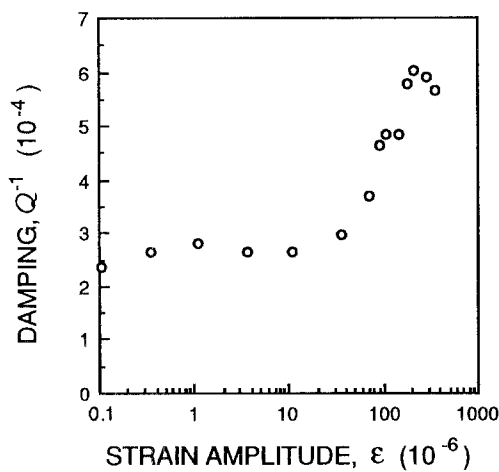


Figure 2 Strain amplitude dependence of damping at room temperature for 99.999% aluminium showing classical dislocation damping trends.

damping and modulus for each strain level. The resonant period and, as a result, the modulus, remained constant throughout the test for all test temperatures used (modulus independent of strain level over the strain range covered). The modulus values from tests performed at different temperatures were then used to determine the temperature dependency of the modulus.

In this study, the Al/Al₂O₃ specimens with 30 vol % fibre and the pure Al specimen were tested from room temperature up to 475°C. All other specimens were tested at room temperature only. The frequency of vibration, determined by the length of the quartz crystals, was 80 kHz for this study.

3. Results and discussion

3.1. Pure aluminium (99.999%)

The results for the tests of the pure Al will be discussed first to establish some baseline trends and allow a more detailed discussion of the Granato–Lücke (GL) theory for dislocation damping [1, 2].

3.1.1. Temperature dependence of modulus in aluminium

Measurement of the dynamic modulus of aluminium at several temperatures from room temperature to 475°C (see Fig. 3) revealed a highly linear loss of modulus with increasing temperature over this temperature range. A linear regression analysis of the data resulted in the correlation

$$E = 73.49 - 0.083 T \quad (R = 0.990)$$

with T in °C, E in GPa, and R as the correlation coefficient. For this aluminium sample the rate of modulus change as a function of temperature, dE/dT , was $-83 \text{ MPa } ^\circ\text{C}^{-1}$.

3.1.2. Classical GL damping behaviour in aluminium

The results for the strain amplitude dependence of mechanical damping at room temperature for the pure Al are shown in Fig. 2. The data followed the classical trends predicted by the GL theory. The GL theory considers a network of dislocation lines with the dis-

location lines pinned by both breakable and unbreakable pinning points. The average distance between unbreakable pinning points is the network length (L_N), while the average distance between breakable, or minor, pinning points is the minor pinning length (L_c). According to the GL theory, the damping mechanism operates as follows. When the material is set into vibration, the dislocation lines vibrate between the pinning points like the strings of bows. At low strain amplitudes, the dislocation line segments vibrate between minor pinning points and their contribution to the overall damping level of the material is essentially constant with strain amplitude. This is termed the amplitude independent region and corresponded to the region of strains less than 10^{-5} for the aluminium specimen. At higher strain amplitudes, a breakaway threshold stress or strain is reached and the dislocation line segments begin to break away from the minor pinning points and cause a damping increase through a hysteretic loss. The hysteretic loss arises from the segments becoming repinned and breaking away again on each stress reversal. This region of nonlinear dependency of damping on strain amplitude is termed the amplitude dependent region and occurred at strains above 10^{-5} in the pure Al test sample.

The transition from the level of damping in the amplitude independent region to the maximum damping level occurred over a range of strains. This was due to there being a distribution of pinning lengths and breakaway threshold levels in the specimen, resulting in a distribution of strain levels at which dislocation segments began to operate in the breakaway mode. In addition, a distribution of strain existed in the specimen which ranged from zero at the ends to a maximum at the centre (node of vibration).

Additionally, the data in Fig. 2 show a loss of damping after the maximum level is reached. Such a peak in the damping capacity in relatively pure metals has been interpreted by Rogers [5] as a demonstration of re-pinning of dislocation line segments by pinning points away from the original pinning points. In other words, a segment bows out far enough at the higher strain amplitudes to become pinned by other points which deactivates the hysteresis loss for this particular dislocation segment.

Analysis of the amplitude dependent portion of the curve in terms of GL theory allowed estimates to be made for L_c and the mobile dislocation density (Λ) in the material. First, an educated estimate of L_N in the material was made. Considering the relatively large grain size for aluminium, a value of $100 \mu\text{m}$ was chosen for L_N . Analysis by the GL theory then yielded values of 10^{-8} m for L_c and 10^9 m^{-2} for Λ . The calculated value for Λ was of reasonable magnitude for a high-purity polycrystalline metal. The number of pinning points per dislocation network length (L_N/L_c) was, on average, 10^4 . This seemed to be a large value, but the following calculation on purity of the metal was consistent with this value.

The average number of pinning points per network length calculated for high-purity aluminium should be related to the level of impurities in the metal. In this

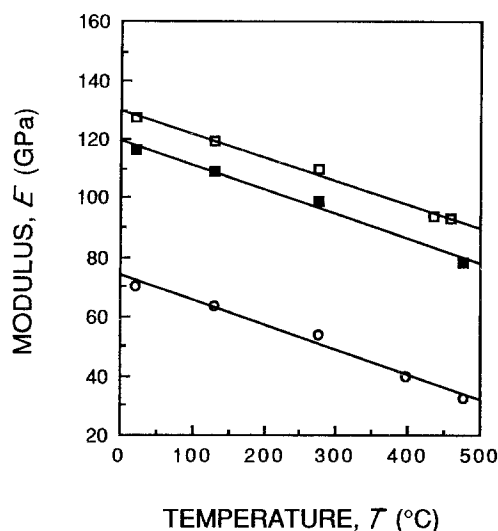


Figure 3 Temperature dependence of dynamic Young's modulus for Al/Al₂O₃ specimens with 30 vol% fibre (□) continuous or (■) chopped) and (○) for 99.999% aluminium.

case, 99.999 wt % purity corresponded to an impurity level of 10 wt p.p.m. The value of L_c , when inverted and cubed, yielded the number of impurity atoms per cubic metre, namely 10^{24} impurity atoms/m³. Using Avogadro's number and the density of aluminium, an impurity level 16 at.p.p.m. was determined. Considering that the identity of the impurity atoms was unknown, it could be said that 10 wt p.p.m. and 16 at.p.p.m. were in good agreement with each other. Therefore, it was concluded that the value of L_c calculated for aluminium with the GL theory was reasonable.

3.2. Aluminium/alumina (Al/Al₂O₃)

3.2.1. Temperature dependence of modulus in Al/Al₂O₃

Fig. 3 shows the temperature dependence of dynamic Young's modulus for the Al/Al₂O₃ MMC with 30 vol% fibre (chopped and continuous). For comparison purposes, the data for pure Al are also included. Linear regression analysis of the Al/Al₂O₃ data yielded the following correlations:

$$\text{continuous fibres: } E = 129.91 - 0.080 T \\ (R = 1.00)$$

and

$$\text{chopped fibres: } E = 119.65 - 0.084 T \\ (R = 0.99)$$

The rate of modulus loss as a function of temperature for these specimens was highly linear. It is noteworthy that the modulus of these MMCs at 475°C exceeded the value for aluminium at room temperature (about 70 GPa).

When the temperature dependence of the modulus of Al/Al₂O₃ was compared to that for aluminium, it was noted that the values of dE/dT for these materials were nearly identical (ranged from -80 to -84 MPa °C⁻¹). Therefore, the decrease in modulus in Al/Al₂O₃ as temperature increased was attributed to the reduction in modulus of the aluminium matrix, not the alumina fibre. The explanation for this can be

sought in terms of the melting points and, hence, the strengths of the interatomic bonds for each constituent. Aluminium melts at the relatively low temperature of 660°C, whereas alumina, being a refractory material, melts at a much higher temperature. Hence, the weakening of interatomic forces (and stiffness) as the temperature increased was expected to be much more pronounced for aluminium than for alumina. In addition, the values of $(-1/E(0))(dE/dT)$, where $E(0)$ is the modulus at 0°C, were 6.16×10^{-4} , 7.02×10^{-4} , and 11.3×10^{-4} °C⁻¹ for Al/Al₂O₃ with continuous fibres, Al/Al₂O₃ with chopped fibres, and pure Al, respectively. These values are in the range documented by Friedel [6] for several pure metals, namely 4 to 14×10^{-4} °C⁻¹, indicating that the processes leading to modulus loss in the samples in this study were predominantly those that occur in metallic materials (aluminium matrix in this case).

3.2.2. Strain amplitude dependence of damping in Al/Al₂O₃

Fig. 4 shows the strain amplitude dependence of mechanical damping for several Al/Al₂O₃ specimens. The overall level of damping for these specimens was low, near 10^{-4} , similar to that for many common metals and alloys. The data indicated that the damping was independent of strain amplitude up to a strain level of approximately 3×10^{-5} . Above this strain level, the damping appeared to be mildly dependent on strain amplitude, except for the 30 vol%, continuous fibre sample.

A close examination of Fig. 4 revealed a trend of higher damping as the volume fraction of alumina decreased. This suggested that the matrix was the major contributor to damping in that, as the volume fraction of the matrix increased (reduced volume fractions of alumina fibre), the overall damping capacity of the material increased. Apparently, increasing the amount of fibre/matrix (FM) interface area by increasing the fibre volume fraction, which was expected to increase dislocation densities, was not an effective means by which to increase damping in Al/Al₂O₃ MMCs.

It should also be noted that the damping level for the specimen with chopped fibres (30% fibre volume fraction) was definitely lower than the level for the specimen with continuous fibres, but showed a greater amount of amplitude dependent damping. The reason for the decreased damping in the chopped fibre sample is not clear, but the amplitude dependent behaviour may be explained in terms of greater dislocation densities. It is possible, though not confirmed for these specimens, that the presence of chopped fibres may have resulted in increased dislocation densities relative to those in continuous fibre specimens (of the same volume fraction) by virtue of the sharp discontinuities at the ends of the fibre segments. The increased dislocation density could then have led to the more pronounced amplitude dependent damping behaviour.

3.2.3. GL analysis for Al/Al₂O₃

The amplitude dependent damping results for the Al/Al₂O₃ specimens in Fig. 4 were analysed in terms of

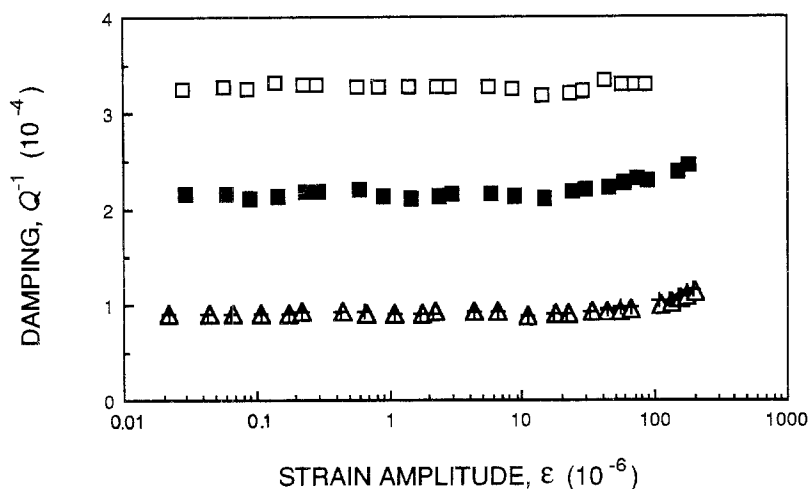


Figure 4 Strain amplitude dependence of damping at room temperature for Al/Al₂O₃ specimens with different fibre vol %: (□) 30, (■) 30 chopped, (△) 45, (+) 55.

the GL theory to estimate the average value of the minor pinning lengths and the mobile dislocation densities. For an estimate of the network length, the fibre spacing, or the average distance between adjacent fibre surfaces, was considered. It was assumed that the fibres themselves acted as unbreakable pinning points for the dislocation lines. Simple calculations for a square array, centred square array, or hexagonal array of circular cross-section fibres (20 μm diameter) yielded average fibre spacings in the range of 12 to 26 μm for the 30 vol % specimens, 6 to 17 μm for the 45 vol % specimens, and 4 to 14 μm for the 55 vol % case. Also, considering that 10 μm is a reasonable estimate for the order of magnitude of aluminium grain sizes in these specimens, a value of 10 μm was used for the network length. The GL analysis then yielded values of $9 \times 10^{-9} \text{ m}$ and $2 \times 10^{11} \text{ m}^{-2}$ for the minor pinning length and the mobile dislocation density, respectively. Thus, the number of minor pinning points per network length was about 1000, which was a reasonable result when compared to previous results from Granato and Lücke [1, 2].

The estimated mobile dislocation density value was, on first consideration, rather high for a nominally annealed material. However, Hartman *et al.* [7] used the GL theory recently to analyse the damping-strain amplitude data for several metal matrix composites and found estimated dislocation densities as high as 10^{15} m^{-2} , very large values for nominally annealed materials. On the experimental side, Arsenault and Fisher [8] used high-voltage transmission electron microscopy (TEM) to examine the regions near the FM interface in MMCs and found very high dislocation densities. They attributed the high dislocation densities to the thermal stresses that were induced during the cooling stage of the fabrication process. Therefore, the estimated values of dislocation density in Al/Al₂O₃ seemed to agree with the estimates in previous work and to the measured values from TEM analysis.

The estimated dislocation densities for Al/Al₂O₃ were two orders of magnitude higher than the estimate for the aluminium sample, yet the damping levels were lower and the amplitude dependent behaviour characteristic of dislocation damping was suppressed. It appears that the presence of the alumina fibres increased the dislocation density, but the dislocation

segments were strongly pinned and unable to provide significant additional damping.

3.3. Aluminium/tungsten (Al/W)

3.3.1. Strain amplitude dependence of damping in Al/W

The strain amplitude dependence of the mechanical damping for the Al/W MMCs is shown in Figs 5 and 6. All specimens exhibited damping trends predicted by GL theory. Fig. 5 examines the effect of the tungsten fibre diameter on the damping behaviour, while Fig. 6 shows the effect of fibre volume fraction. As discussed in a previous paper by Wolfenden and Wolla [9], changes in the fibre diameter (at constant fibre volume fraction) had a more pronounced effect on the damping behaviour than did volume fraction changes (at constant fibre diameter).

From Fig. 5, it is apparent that for Al/W specimens with similar fibre volume fractions, larger fibre diameters resulted in: (a) higher damping levels in the strain amplitude independent region, (b) initiation of the amplitude dependent region behaviour at lower strain levels, and (c) greater rates of increase in damping capacity in the amplitude dependent region. The accuracy and sensitivity of the PUCOT strain measurement permitted the determination of the strain levels at which the amplitude dependent behaviour commenced (approximately 4×10^{-6} for 0.127 mm fibres, 3×10^{-6} for 0.305 mm fibres, and 2×10^{-6} for 0.762 mm fibres).

Conflicting correlations for the effect of variations in the fibre volume fraction were observed with higher damping levels as the volume fraction increased in the 0.127 mm diameter fibre case (Fig. 5) and lower damping levels as the volume fraction increased in the 0.305 mm diameter case (Fig. 6). Because variations between specimens from different manufacturers (0.127 mm case) could have affected the results in an undetermined manner, and the results for the 46 and 55 vol % specimens (0.305 mm case) were within the experimental uncertainty of each other, no conclusive statement could be made regarding the effect of the fibre volume fraction on damping levels in these specimens.

The trend of increasing damping level with increasing fibre diameter should be examined further. Note that the damping levels for all Al/W specimens were higher than the level measured for the aluminium

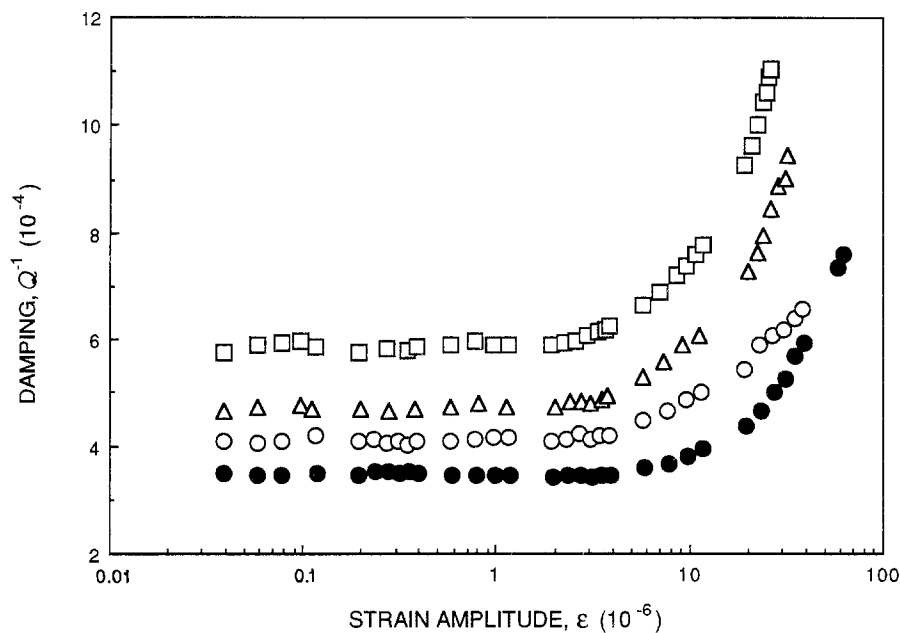


Figure 5 Strain amplitude dependence of damping at room temperature for Al/W specimens with similar fibre vol % and different fibre diameters. (\square) Al/50 W (0.762), (Δ) Al/46 W (0.305), (\circ) Al/50 W (0.127), (\bullet) Al/44 W (0.127).

sample. This could indicate that the increased damping in Al/W was due to the interaction between the fibre and matrix, the presence of the tungsten fibre itself, or a combination of both. If dislocation motion at the FM interface was the main contributor to damping in these materials, then the observations of Arsenault and Fisher [8], that there was an increased dislocation density in the vicinity of the fibres in MMCs, become important here. It could be considered that the fibre diameter and the resulting interfibre spacing and FM interface area helped to determine the quality of the interface between the matrix and the fibre, as well as the magnitude of the thermally induced stresses which generated dislocations during the cooling stage of fabrication. These effects need to be studied with careful TEM analysis of MMCs. It is likely that the fibre volume fraction, interfibre spacing, fibre diameter, and FM interactions all affect the damping by influencing the dislocation density.

As mentioned above, it is possible that the tungsten fibre itself was largely responsible for the damping, rather than the interaction of the fibre with the matrix. The trends noted here showed higher damping for Al/W MMCs with larger fibre diameters (volume fraction held constant) and, therefore, the amount of interface area between the fibre and matrix lower. The effect of FM interface area on dislocation densities becomes a lesser concern if the dislocation density within the fibre is the controlling factor. Again, TEM work is needed to clear up some of these uncertainties.

3.3.2. GL analysis for Al/W

To apply the GL theory to the data in Figs 5 and 6, the interfibre spacing for the Al/W specimens was estimated as it was for the Al/FP specimens. For the three fibre packing arrays considered and the fibre volume fractions and diameters present, the range of interfibre spacings was 32 to 589 μm . Typical grain sizes in the

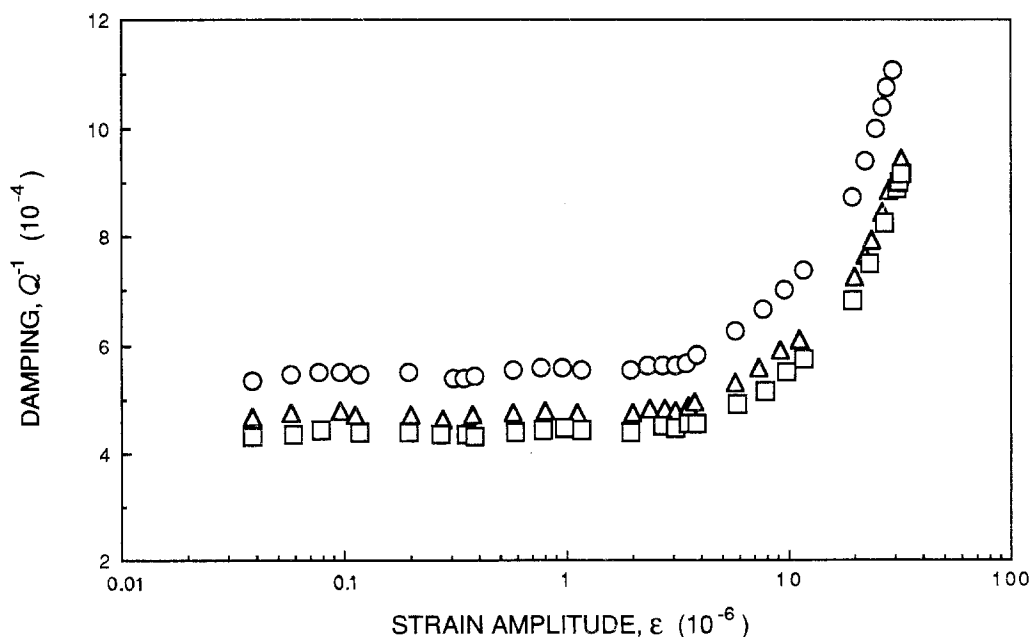


Figure 6 Strain amplitude dependence of damping at room temperature for Al/W specimens with different fibre vol % of the same diameter fibre. (\circ) Al/37 W (0.305), (Δ) Al/46 W (0.305), (\square) Al/55 W (0.305).

TABLE II Minor pinning lengths and dislocation densities for Al/W specimens with an estimated network length of 10 μm

Specimen ID	Pinning length, L_c (10^{-10} m)	Dislocation density, Λ (10^{11} m $^{-2}$)	Pinning points per network length
Al/44W (0.127)	349	3	286
Al/50W (0.127)	604	5	165
Al/37W (0.305)	741	14	135
Al/46W (0.305)	742	10	135
Al/55W (0.305)	688	8	145
Al/50W (0.762)	890	11	112

aluminium matrix for these materials were estimated to be on the order of 10 μm and, because this would be the limiting dimension, it was chosen for the network length. The GL analysis then yielded the values for the minor pinning lengths and dislocation densities shown in Table II. The number of pinning points per network length varied from about 100 to 300, which was reasonable [1, 2]. The estimated dislocation densities were reasonable for an annealed material.

Examining the results for the 0.127 mm fibre diameter specimens (specimens from different manufacturers), it is apparent that processing conditions had a significant influence on the pinning lengths. The different processing conditions could have led to differences in the final composition and grain structure of the constituents which affected the pinning lengths. Concentrating on specimens from the same manufacturer with the same processing conditions, some trends can be seen. For specimens with 0.305 mm diameter fibres, the pinning length remained relatively constant (near 7×10^{-8} m) while the dislocation density decreased as the fibre volume fraction increased. There appeared also to be a trend of both increasing pinning length and dislocation density as the fibre diameter increased in specimens of similar volume fraction. Each of these trends went against the reasoning that increased FM interface area will result in increased dislocation density and suggests that the tungsten fibre itself may be the dominant influence on the overall damping behaviour. In fact, when a network length of 1 μm was used in the GL analysis, with 1 μm being a reasonable estimate for the grain size in drawn tungsten fibres, the calculated dislocation densities increased by three orders of magnitude. The large dislocation densities in this case might explain the increased damping levels in Al/W over those in aluminium and the strong amplitude dependent behaviour that was observed. Again, the actual circumstances were very complex and TEM analysis is needed to understand better what is controlling the damping behaviour.

4. Conclusion

Several observations can be made from the present study of the mechanical damping and dynamic Young's modulus of Al/Al₂O₃ and Al/W performed with the PUCOT at 80 kHz and at temperatures up to 475°C. First, the specific materials will be examined, and then some general conclusions will be stated.

For Al/Al₂O₃, it was found that the modulus increased, as expected, with the addition of the alumina fibres. The modulus loss with increasing tem-

perature was highly linear in the 30% fibre volume fraction case with the modulus loss attributed mostly to the aluminium matrix, not the fibre. The reinforcing effect of the fibre addition was sufficient to keep the modulus measured for the composite at 475°C higher than the modulus value at room temperature for aluminium. The presence of the alumina reduced the measured damping levels and suppressed the amplitude dependent portion of the damping response. Estimated dislocation densities in Al/Al₂O₃ were high, yet damping attributable to the dislocation damping mechanism was not observed, suggesting that the dislocations were well-pinned. The possibility that chopped fibre samples may achieve higher dislocation densities and lead to higher intrinsic damping while maintaining high modulus was indicated.

The Al/W specimens exhibited GL dislocation damping behaviour with high dislocation densities, but some conflicting trends between interface area and damping were observed and need to be studied further. In particular, specimens with larger fibre diameters, and, therefore, less FM interface area (considering specimens with similar fibre volume fractions), had higher dislocation densities, higher damping levels, and a more pronounced dislocation damping behaviour. The situation was quite complex, but increasing the FM interface area clearly did not translate into increased damping capacity for these composites. The possibility exists that the tungsten fibre itself contributed the increased dislocation density and dominated the damping behaviour through dislocation damping.

In comparing these materials under study, it should be noted that the levels of damping in the amplitude independent regions were within a factor of five of each other and too low for practical damping applications. It appears, therefore, that while augmenting the *modulus* by fibre addition was realized, augmenting the *damping* capacity in aluminium by adding fibres such as tungsten and alumina had limitations. On the other hand, significant increases in the damping of Al/W were found in the amplitude dependent region and, with further study and understanding of the mechanism by which this occurs, the possibility exists for improving the intrinsic damping of these materials, while maintaining the modulus and strength.

References

1. A. GRANATO and K. LÜCKE, *J. Appl. Phys.* **27** (1956) 583.
2. *Idem, ibid.* **27** (1956) 789.

3. W. H. ROBINSON and A. EDGAR, *IEEE Trans. Sonics and Ultrasonics* **SU-21** (1974) 98.
4. A. WOLFENDEN and M. R. HARMOUCHE, *J. Mater. Sci.* **20** (1985) 654.
5. D. H. ROGERS, *J. Appl. Phys.* **33** (1962) 781.
6. J. FRIEDEL, in "Dislocations" (Pergamon Press, New York, New York, 1964) App. B, p. 454.
7. J. T. HARTMAN JR., K. H. KEENE, R. J. ARMSTRONG and A. WOLFENDEN, *J. Metals* **38** (1986) 33.
8. R. J. ARSENAULT and R. M. FISHER, *Scripta Metall.* **17** (1983) 67.
9. A. WOLFENDEN and J. M. WOLLA, "Proceedings of the 19th International SAMPE Technical Conference" (SAMPE, Covina, California) p. 37.

*Received 27 June
and accepted 8 December 1989*